Bubble dynamics and heat transfer for pool boiling on hydrophilic, superhydrophobic and biphilic surfaces

E. Teodori[1], **T. Palma**[1], **T. Valente**[1], **A.S. Moita**[2], **A.L.N. Moreira**[1]
[1,2]IN+ - Center for Innovation, Technology and Policy Research, Instituto Superior Técnico, Universidade de Lisboa, Av. Rovisco Pais, 1, 1049-001 Lisboa, Portugal

E-mail: anamoita@dem.ist.utl.pt

Abstract. This paper proposes a detailed analysis of bubble dynamics to describe pool boiling heat transfer in extreme wetting scenarios (superhydrophobic *vs* hydrophilic). A mechanistic approach, based on extensive post-processing allows quantifying the relative advantage of the superhydrophobic surfaces to endorse the onset of boiling at very low superheats (1-2K) *vs* their worse heat transfer performance associated to the swift formation of an insulating vapour film. Based on this analysis, a simple biphilic surface is created. The results suggest that for high heat fluxes, bubble dynamics is dominated by the emission of very small bubbles, which seems to affect the interaction mechanisms, precluding the emission of the large bubbles from the surface, thus compromising the good performance of the biphilic surfaces.

1. Introduction

Pool boiling heat transfer is a vital process in many industrial applications, thus being a hot research topic for many years. Several studies focus on heat transfer enhancement, mainly searching to increase the heat transfer coefficients and the Critical Heat Flux, by altering the surface properties, mainly surface topography (e.g. [1]) and/or chemistry (e.g. [2]). However, boiling is a complex phenomenon involving several interconnected mechanisms of mass, momentum and energy transfer between liquid-solid-vapour phases, which is far to be completely understood [3-4]. Given that wettability is altered by both surface topography and chemistry, several of the aforementioned studies simultaneously alter surface topography and wettability in a non-systematic way, which precludes the identification of dominating effects. Recognizing the need to separate the effects of altering surface topography and chemistry, recent studies allowed identifying dominating roles of surface topography and wettability: for mild modifications of surface wettability, changing the surface topography mainly acts to promote potential nucleation sites [5], although care must be taken to keep the interaction mechanisms under control. Hence, the potential enhancement of pool boiling heat transfer by altering the surface topography can be overcome by the negative dominating effects of the interaction mechanisms, between nucleation sites and bubbles, which can actually promote the formation of large vapour blankets, strongly declining the heat transfer coefficients and endorsing the occurrence of the critical heat flux at lower wall superheat [6-7]. Under extreme wetting scenarios, surface topography plays a secondary role, being the onset of boiling triggered at very low surface superheat for boiling over superhydrophobic surfaces, which in turn have much lower Critical Heat Fluxes, when compared to

[2] To whom any correspondence should be addressed.

the hydrophilic surfaces [5, 8]. In turn, hydrophilic surfaces require a much larger degree of superheat to start the nucleation, but often allow obtaining higher heat transfer coefficients and Critical Heat Fluxes. Based on this trend, few authors promptly passed on to an "optimum" surface, considering an adequate superhydrophilic/superphydrophobic patterning of the surface – the so-called superbiphilic surfaces [9], mainly based on the evaluation of the heat transfer coefficients. However, the detailed characterization of bubble dynamics and its relation to the heat transfer processes is still scarcely reported in the literature, particularly for these extreme wetting regimes. This is an important step, given that, despite the scepticism of various authors in dealing with the mechanistic approaches, as earlier suggested by [10], important relations between bubble dynamics and heat transfer are recognized to be useful in the description of the heat transfer processes [3] and even to predict Critical Heat Fluxes [11]. Hence, the present paper addresses the characterization of the heat transfer processes under extreme wetting scenarios (hydrophilic vs superhydrophobic surfaces) showing the need to combine both characteristics in the so-called (super)biphilic surfaces. Heat transfer is quantitatively assessed based on the analysis of the boiling curves obtained for the various surfaces, being the results interpreted based on the particular bubble dynamics depicted for the various wetting regimes addressed here. It is worth mentioning that at this stage of the work, emphasis is taken in analysing the bubble dynamics and heat transfer processes, thus the biphilic patterns are not customized to provide the highest heat transfer coefficients, but instead to allow the description of the observed phenomena.

2. Experimental arrangement and methodology

2.1. Experimental arrangement

The experimental rig is mainly composed by a boiling chamber, where the experiments are performed, a degassing system in which the fluid is pressurized and constantly heated and filling and evacuating circuits, being the latter at ambient pressure. The boiling chamber has approximately a cubic shape with 200mm side. The pressure and the temperature inside the boiling chamber are accurately controlled (the temperature is controlled with a precision of 1 K and for the pressure control the precision is 1.6 mbar). Heaters disposed inside and on the outer surfaces of the boiling chamber are controlled by a PID controller to assure that the liquid remains inside the chamber at saturation temperature. A type K thermocouple records the saturation data of the liquid, while a second thermocouple (also type K), located 25mm above the heating surface is used for PID control. The pressure is controlled by means of two electronic valves, which are actuated based on the measures given by a pressure transducer (OMEGA DYNE Inc.) inside the pool, using a home-made software based loop control. This control system reacts to pressure variations in the order of 5mbar. The refilling and the entire measurement processes are automatically controlled by this routine. The temperatures are sampled using type K thermocouples. The signal is acquired and amplified by a National Instruments DAQ board plus a BNC2120. The acquisition frequency is 100Hz. The entire heating block of the pool boiling test section is isolated with Teflon, from the outside and the pool boiling chamber is isolated with rubber. The heating block, which heats and accommodates the different surfaces, comprises a copper cylinder with a diameter of 20mm, inside which a cartridge heater (up to 315W) is placed. The surfaces with dimensions 62x62x1mm^{3}are positioned on the heating block using a custom made system with bolts and springs, to assure the perfect thermal contact. The bolts contacting the surfaces are made from PEEK (polyether ether ketone) to minimize heat that is dissipated from the surface to the bolts. The heat flux is measured using a thin heat flux sensor (Captec Enterprise ®, with a sensitivity of 2.21mV/(W/m^2)) custom made to fit perfectly to the heating block. A more detailed description of the experimental rig is provided in [8].

2.2. Methodology

The test surfaces are characterized by their topography and wettability, being the later quantified based on the quasi-static advancing θ_{adv} and receding angles θ_{rec}, together with the contact angle hysteresis= θ_{adv} - θ_{rec}. Afterwards, pool boiling curves are constructed for each test surface, which are obtained by

slowly imposing the heat flux in small increasing power steps. For each power step, bubble dynamics and nucleation mechanisms are also characterized based on high-speed visualization, using a high-speed camera (Phantom v4.2 from Vision Research Inc.). Quantitative information regarding bubble dynamics is further obtained by image post-processing procedures. The working fluid used is degassed distilled water. The relevant thermo-physical properties are summarized in table 1.

Table 1. Thermo-physical properties of water, taken at saturation at 1.013×10^5 Pa.

Property	Value
Saturation temperature T_{sat} (°C)	100
Liquid density ρ_l (kg/m^3)	957.8
Vapor density ρ_v (kg/m^3)	0.5956
Dynamic viscosity of the liquid μ_l (mN m/s^2)	0.279
Specific heat c_{pl} (J/kgK)	4217
Thermal conductivity k_l (W/mK)	0.68
Latent heat of evaporation h_{fg} (kJ/kg)	2257
Liquid surface tension σ (N/m)x10^{-3}	58

2.2.1. Preparation and characterization of the surfaces

Stainless steel surfaces are prepared to have different topographic and wetting properties, namely to be hydrophilic or superhydrophobic. The superhydrophobic surfaces are obtained at the expense of a chemical coating (a commercial compound called Glaco Mirror Coat Zero, from Soft99 Co, which is mainly a perfluoroalkyltrichlorosilane combined with perfluoropolyether carboxylic acid and a fluorinated solvent). All the surfaces are first cleaned, according to the following main steps: a) 30 min in an ultrasonic bath in water at 40ºC, b) drying with compressed air and c) 30 min in an ultrasonic bath in acetone at 40ºC. Then the coating is applied as in [5]. The aforementioned cleaning procedure must be repeated for each surface and for all the boiling curves. A similar procedure is followed to produce the biphilic surfaces, which are mainly composed by square patterns of hydrophilic and superhydrophobic regions. The squares are 10mm^2.

The homogeneity of surface topography and morphology is checked by Laser Scanning Confocal Microscopy (Leica SP8 Confocal Microscope) using the reflection mode. Then, the stochastic roughness profiles are measured using a Dektak 3 profile meter (Veeco) with a vertical resolution of 20nm. These profiles are further processed to obtain the mean roughness (determined according to standard BS1134) and the mean peak-to-valley roughness (determined following standard DIN4768). Average representative values of R_a and R_z are taken from 10 measurements distributed along the entire surface.

The contact angles are measured at room temperature (20ºC), using an optical tensiometer (TETA from Attention). The angles are evaluated from the images taken within the tensiometer, using a camera adapted to a microscope. The images (with resolution of 15.6 μm/pixel, for the optical configuration used here) are post-processed by a drop detection algorithm based on Young-Laplace equation (One Attention software). The surfaces are characterized as hydrophilic (apparent quasi-static advancing angles lower than 90º) or superhydrophobic (apparent quasi-static advancing angles higher than 150º and hysteresis lower than 10º, following the criteria established in [12]. Table 2 depicts the main characteristics of the categories of surfaces defined for the present study. The contact angles were quite reproducible. The values presented here are taken as an average of 3 representative measurements distributed along the surface. Deviations in R_a were admitted around 10% within each category.

Table 2. Main characteristics of the test surfaces.

Category	Surface material	R_a [μm]	R_z [μm]	θ_{adv} [°]	θ_{rec} [°]	Hysteresis [°]
Hydrophilic	Stainless steel	0.06	0.09	85±1	<20	>10
Superhydrophobic	Stainless steel coated with *Glaco*	0.06	0.09	166±1	164	2

2.2.2. Pool boiling curves

The boiling curves are obtained under imposed heat flux conditions on the surface, with continuous control and monitoring of the surface temperature, liquid temperature and pressure inside the pool boiling chamber. The curves were obtained at 1 bar ± 10mbar for each surface by varying the imposed heat flux in steps. Each curve is averaged from 4 experiments. The uncertainty in temperature measurements is ±1K. The maximum uncertainty in the heat flux measurements is 3.3%. The detailed analysis of the measurement errors and uncertainties is presented in [8].

2.2.3. Bubble dynamics

The characterization of the nucleation mechanisms and bubble dynamics is based on the measurement of several quantities obtained from high-speed visualization and image post-processing. The images are recorded with a frame rate of 2200fps and a resolution of 512x512 pixel^2. For the optical configuration used here, the spatial resolution is 31.85 μm/pixel. A home-made code developed in MATLAB enables determining the temporal evolution of the bubble diameter (until detachment), bubble contact angle, velocity of the bubble centroid, velocity of the contact line and bubble departure frequency. The temporal evolution of bubble growth is measured for each test condition, from the entire bubble growth period until detachment. Then, averaged values are taken, for the instant of bubble detachment, for various detachment events. The maximum relative error when determining the bubble parameters is 10%, as exhaustively analyzed in [6-8].

3. Results and discussion

3.1. Heat transfer and bubble dynamics under extreme wetting scenarios (hydrophilic vs superhydrophobic surfaces)

Changing the wettability within extreme scenarios leads to significant differences in bubble dynamics, covering various phenomena which occur at different temporal and spatial scales. Hence, for water boiling on the hydrophilic surfaces, at low heat fluxes, corresponding to a wall superheat of 21K, the nucleation sites are sparsely located within the heated area (Φ20mm) and very few sites are active. Bubble size remains almost constant, while the emission frequency shows a general decreasing trend. At higher heat fluxes, the bubbles merge into large mushroom shaped vapour slugs and fluid motion becomes chaotic. This behavior contrasts with the boiling process observed on the superhydrophobic surfaces: even at superheat values of 1-2K, an immediate coalescence of bubbles in the near surface region occurs, generating an insulating vapor layer, from which a single big bubble starts to grow and depart from the surface. This behavior is in agreement with the results recently reported by [5]. This boiling morphology remains mostly unchanged at higher imposed heat fluxes, except for an increase of the bubble size and emission frequency. The detailed visualization of the morphology described above is depicted in [8]. The insulating vapor layer, together with the particular bubble dynamics discussed in the previous paragraphs can also be roughly evaluated considering the heat transfer mechanisms. In fact considering the mechanistic approach of the RPI model [10], the heat flux removed from the surface can be taken as a sum of three main contributions: the heat transferred by natural convection $q"_{nat\ conv}$, the latent heat removed by liquid vaporization during bubbles formation $q"_{vap}$ and the heat removed by quenching $q"_{q}$, i.e. by the disruption of the thermal boundary layer as the

bubbles detach from the surface, followed by the surface re-wetting by the liquid. These terms can be estimated as:

$$q''_{natconv} = \left[1 - \frac{\pi}{4A}\sum_{n=1}^{N_T}\left(D_{b,n}\right)^2\right] h_{natconv}\left(T_w - T_{sat}\right) \quad (1)$$

$$q''_{vap} = \frac{\pi}{6A}\rho_v h_{fg}\sum_{n=1}^{N_T}\left(f_b . D_b^3\right) \quad (2)$$

$$q''_q = \frac{2\pi k_l (T_w - T_{sat})}{A\sqrt{\pi\alpha_l}}\sum_{n=1}^{N_T}\left(D_b^2 . \sqrt{t_{wn}}\, f_b\right) \quad (3)$$

Here, A is the area of the heater, N_T is the total number of active nucleation sites, t_{wn} is the waiting time and $\alpha_l = k_l/\rho_l C_{pl}$ is the liquid thermal diffusivity. $h_{natconv}$ can be estimated considering a typical correlation for natural convection on a horizontal plate (e.g. McAdams correlation, as suggested by [13]). Average values of the bubble dynamic parameters, such as the departure diameter and frequency can be provided by intensive image analysis, whose procedures and associated errors are summarized in section 2. While the relative weight of the heat removed by natural convection is typically lower than 30%, the terms associated to bubble vaporization and quenching are dominant [13]. For illustrative purposes one can estimate the term associated to the vaporization of the bubbles q''_{vap} following eq. (2), for the particular conditions summarized in table 3:

Table 3. Bubble dynamics parameters for vaporization rate analysis.

Surface	Wall superheat (K)	$q''_{measured}$ (W/cm^2)	Bubble departure diameter D_b (mm)	Bubble departure frequency f_b (Hz)	Active nucleation sites
Hydrophilic	27	4.88	3.25	15.21	21
Superhydrophobic	32	1.1	9.17	7.75	1

For these conditions, the vaporization rate is $3.51\text{x}10^{-3}$g/s for the hydrophilic surface and $1.86\text{x}10^{-3}$g/s for the superhydrophobic surface. There are, naturally, many issues in this estimation considering the equivalent conditions for the evaluation of the vaporization rate, given the subjective nature of accounting average parameters for multiple nucleation sites, as occurs for the case of the hydrophilic surface. So this analysis mostly deserves a qualitative interpretation. However, for similar superheating conditions these results allow identifying trends. Hence, the vaporization rate is much lower for the superhydrophobic surface, as the insulating vapor layer will preclude the heat transfer from the surface to the liquid, thus limiting the vaporization rate. On the other hand, the fact that the large bubble stays attached to the surface for longer periods of time, significantly reduces the bubble emission frequency for the superhydrophobic surface, further contributing to the lower value of the vaporization rate obtained.

The estimation of the value of the heat flux removed by vaporization for the hydrophilic surface as given by eq. (2) is almost half of the total amount of the heat flux that was measured by the sensor (me_{asured} depicted in table 3). This can be related to the strong weight of the term associated to the heat removed by the quenching mechanism. The current experimental conditions do now allow a reliable estimation of the waiting time and consequently of this term, as given by eq. (3). Nevertheless, this difference is in agreement with the estimations of [13], who evaluate the quenching term to be at least of the same magnitude of the $q''_{vap.}$. For the superhydrophobic surface instead, the presence of the

vapor layer precludes the occurrence of quenching, so following the same reasoning, the heat flux removed by vaporization is very close to the measured one.
Based on these arguments, the heat flux removed from each of these surfaces, as a function of the wall superheat should follow the trend depicted in figure 1.

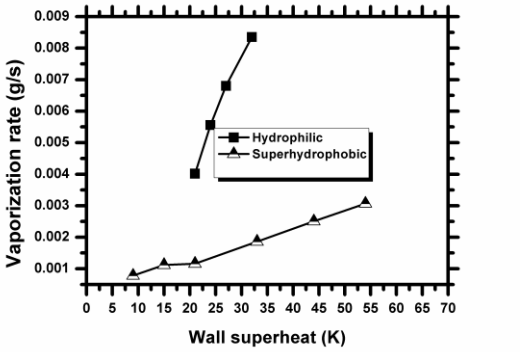

Figure 1. Vaporization rates for hydrophilic and superhydrophobic surfaces as a function of wall superheat.

From the results depicted in this figure and supported by the discussion performed up to now, the superhydrophobic surface starts to vaporize liquid at a much lower wall superheat, when for the hydrophilic surface the heat is only transferred by natural convection. Hence, for lower surface superheat values, one may argue that higher heat flux is removed from the superhydrophobic surface, for similar superheat values, when compared to the hydrophilic one. This should be further confirmed by the experimental results, refining the measurements, to try capturing the boiling incipience point, which was not possible for the accuracy available in the present set-up.
As the wall superheat increases and the insulating vapor layer is generated over the superhydrophobic surface, the heat that is transferred from the surface to the liquid is strongly limited, so the heat flux removed for the same wall superheat becomes much lower, when compared to that obtained for the hydrophilic surface.

3.2. Characterization of biphilic surfaces
Considering the differences between wetting scenarios analyzed in the previous paragraphs, one may try to take advantage of the particular features of each scenario aiming at optimizing the boiling phenomena and the heat flux removed. For instance, as aforementioned, the minimum energy barrier for the onset of boiling is easily transposed for superhydrophobic surfaces [4], but then the force balance retains the bubbles attached to the surface, leading to coalescence and formation of a film from which the large single bubble departs, which constrains the heat transfer mechanisms, as quantified in the previous paragraphs. Hence, the resulting boiling curve, as depicted in figure 3 confirms that the onset of boiling occurs during the first power step, at about 1-2K of wall superheat. Afterwards, the heat flux increases almost linearly with surface superheating, with much lower slope than that of the hydrophilic surface. This is the so-called “quasi-Leidenfrost” phenomenon, identified in [5] and later confirmed in [8]. Combining the two wetting regimes into a biphilic surface may actually increase the boiling heat transfer, as proposed for instance by [9]. In fact, during preliminary experiments performed in the present work, there was a coating failure which led to the appearance of hydrophilic spots on a superhydrophobic surface, which in turn led to a significant increase of the heat flux removed, as depicted in figure 2. This result is in agreement with those reported in [9], although it is not perfectly clear which were the processes behind this significant enhancement in the heat transfer. The analysis performed up to now suggests a vital role of bubble dynamics on the enhanced heat transfer obtained with the biphilic surfaces. To infer on this, a very simple biphilic surface was created with a pattern of 10mm side squares varying between superhydrophobic and hydrophilic

regions and experiments were performed to obtain the respective boiling curve and high-speed visualization of the boiling phenomena.

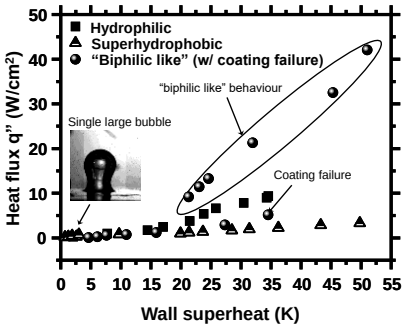

Figure 2. Boiling curves evidencing a "biphilic like" behaviour (with coating failure).

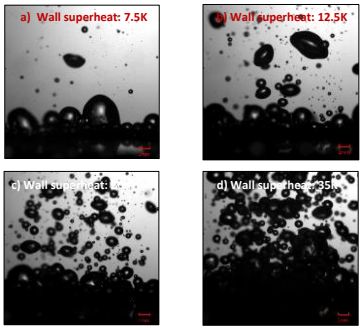

Figure 3. Bubble dynamics on a biphilic surface.

The onset of boiling was achieved, for this biphilic surface at about 7.5K wall superheat (figure 3a), which is in between the onset of boiling wall superheat for the superhydrophobic surface – ≈2 K – and for the hydrophilic one – ≈14 K. At this initial temperature, there is very little bubble emission, although the boiling morphology already depicts hybrid characteristics between hydrophilic and superhydrophobic regimes. Hence, large bubbles stay attached to the surface, mostly at the superhydrophobic regions, but then random releases of very small bubbles can be observed over the entire surface, as illustrated in figure 4a. As the wall superheat increases up to 12.5K (figure 3b), the attached larger bubbles start to be released from the surface. Simultaneously, the emission of the very small bubbles is increased. However, further augmenting the wall superheat, the emission of the small bubbles increases steeply, which in turn reduces the emission of the larger bubbles that stay again attached to the surface (figure 3c). This dominance of the small bubble emission which is very clear in figure 3d, may be related to interaction mechanisms, although additional research is now required. This qualitative description of bubble dynamics for the biphilic surface is quantitatively represented in figure 4.

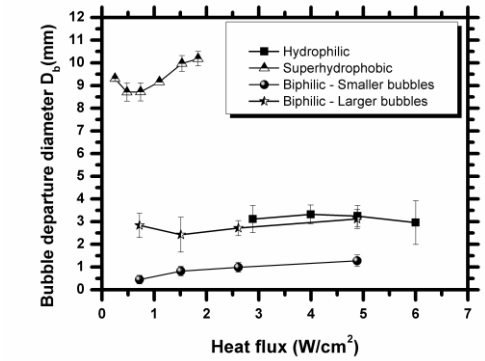

Figure 4. Bubble dynamics for the biphilic patterned surface.

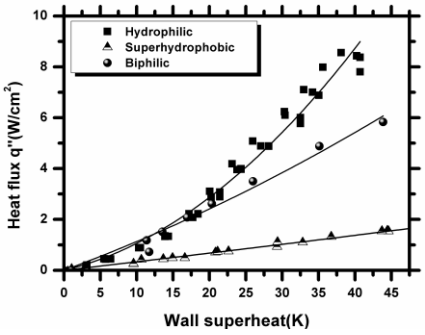

Figure 5. Boiling curves for water on all the surfaces tested in this work.

It is worth mentioning that the larger bubbles generated on the biphilic surface are still smaller than those observed on the hydrophilic one, which contributes to the overall higher heat flux that is removed from the biphilic surface at low wall superheats, as shown in figure 5. Nevertheless, it is clear from figure 5 that, even with earlier point of boiling incipience, there is a significant reduction of the heat flux at higher superheat for the biphilic surface when compared with the hydrophilic one, which can be probably related to the particular bubble dynamics observed: the increased emission of very

small bubbles may not be enough to overcome the reduced heat transfer which occur when the large bubbles remain attached on the surface (which is in agreement with the analysis performed in section 3.1). However, this biphilic surface was created for visualization purposes alone, so the biphilic patterns must be optimized to produce effective surfaces with improved heat transfer performance.

4. Final remarks

The present paper addresses the description of the pool boiling heat transfer mechanisms, based on the detailed analysis of bubble dynamics for water on surfaces with extreme wetting scenarios (superhydrophobic vs hydrophilic regimes). The superhydrophobic surfaces created here evidence a peculiar bubble dynamics behavior which endorses the onset of boiling at very low superheats (1-2K), but then a large insulating vapor film covers the entire surface, leading to the emission of single large bubbles. A mechanistic approach, making use of experimental data obtained by visualization and extensive post-processing analysis allows quantifying the strong constrain in the heat transfer from the surface to the liquid due to this peculiar bubble dynamics. Based on this analysis, a simple biphilic surface is created with large square patterns of superhydrophobic/hydrophilic regions. The results, comprising boiling curves and bubble dynamics are qualitatively in agreement with the few studies reported in the literature on the development of biphilic surfaces. Hence, the onset of boiling in these surfaces is observed for wall superheat values located between those obtained on hydrophilic and superhydrophobic surfaces, respectively, which is in agreement with the bubble dynamic characteristics evaluated in the present work. However, care must be taken for high heat fluxes, as bubble dynamics is dominated by the emission of very small bubbles, which despite being potentially beneficial for the heat transfer, seems to affect interaction mechanisms, precluding the emission of the large bubbles from the surface, thus compromising the good performance of the biphilic surfaces.

Acknowledgements

The authors acknowledge to Fundação para a Ciência e a Tecnologia (FCT) for partially financing the research under the framework of the project RECI7EMS-SIS/0147/2012 and for supporting T. Valente with a research fellowship. The authors are also grateful to FCT for financing AS Moita with a Post-Doc fellowship (SFRH/BPD/109260/2015) and E. Teodori with a PhD fellowship (SFRH/BD/88102/2012).

References

[1] Nimkar D N, Bhavnani S H and Jaeger R C 2006 *Int. J. Heat Mass Transfer* **49** 2829
[2] Takata Y, Hidaka S and Hu L 2006 *Heat Transf.* Eng. **27** 25
[3] Kim J 2009 *Int. J. Multiphase Flow* **35** 1067
[4] Moreira ALN 2014 Multiscale interfacial phenomena and heat transfer enhancement *Proc. 14th Int. Heat Transf. Conf. (Kyoto, Japan, 10-15 August 2014)*
[5] Malavasi I, Bourdon B, Di Marco P De Coninck J. and Marengo M 2015 *Int. Comm. Heat Mass Transf.* **63** 1
[6] Teodori E, Moita AS and Moreira ALN 2013 *Int. J. Heat Mass Transf.* **66** 261
[7] Moita AS, Teodori E and Moreira ALN 2015 *Int. J. Heat Fluid Flow* **52** 50
[8] Valente T, Malavasi I, Teodori E, Moita AS, Marengo M and Moreira ALN 2015 Effect of extreme wetting scenarios on pool boiling *Proc. UK Heat Transfer Conference, UKHTC 2015 (Edinburgh, UK, 7-8 September 2015)*
[9] Betz A, Jenkins J, Kim C and Attinger D 2013 *Int. J. Heat Mass Transf.* **57** 733
[10] Kurul N and Podowski M 1990 *Proc. Int. Heat Transf. Conf.* **1** pp 21-25
[11] Kandlikar SG 2001 *J Heat Transf.* 2001 **123** 1071
[12] Bushan B and Jung Y 2011 *Prog. Material Sci.* **56** 1
[13] Gerardi C, Buongiorno J, Hu L-w and McKrell T 2010 *Int. J. Heat Mass Transf.* **53** 4185